Wrocław University of Environmental and Life Sciences

epos pl

EGU General Assembly 2020

High-rate GNSS positioning for tracing anthropogenic seismic activity

Iwona Kudłacik [1], Jan Kapłon [1], Grzegorz Lizurek [2], Mattia Crespi [3] and Grzegorz Kurpiński [4]

For questions: iwona.kudlacik@upwr.edu.pl

[1] Institute of Geodesy and Geoinformatics, Wrocław University of Environmental and Life Sciences, Poland
[2] Institute of Geophysics, Polish Academy of Sciences, Poland
[3] Geodesy and Geomatics Division, DICEA-Sapienza University of Rome, Italy
[4] KGHM CUPRUM Sp. z.o.o. – Research and Development Centre, Poland

Introduction

High-rate GNSS observations are used in applications that require high precision and information about changes in the location of GNSS stations in small time intervals, such as earthquake monitoring, including early warning systems, and structural health monitoring.

Here, we aimed to present **the novel application of GNSS-seismology broadening its usefulness to the mining areas**. The subcentimetre vibrations caused by anthropogenic seismic activity might be successfully tracked via high-rate GNSS stations.

GNSS		SM			DISTANCES [km]		
SITE	FREQ. [Hz]	SITE	FREQ. [Hz]	ORIGINAL UNIT	GNSS/SM	GNSS/EPIC	SM/EPIC
LES1	10	KOMR	250	m/s^2	0.002	2.52	2.52
TRZB	10	TRBC2	250	m/s^2	0.045	0.97	1.00
TARN	10	TRN2	100	m/s	0.316	3.27	3.26

Table 1: Details of co-located high-rate GNSS and strong-motion (SM) stations.

Data

The most prominent mining tremor event that has been recorded was in the area of Legnica-Głogów Copper District on 29 January 2019 (12:53:44 UTC), with a magnitude of 3.7. The epicentre was located at 51.51°N, 16.12°E, with a hypocentral depth of 800 m, a source radius of over 300 m and a cavity collapse mechanism.

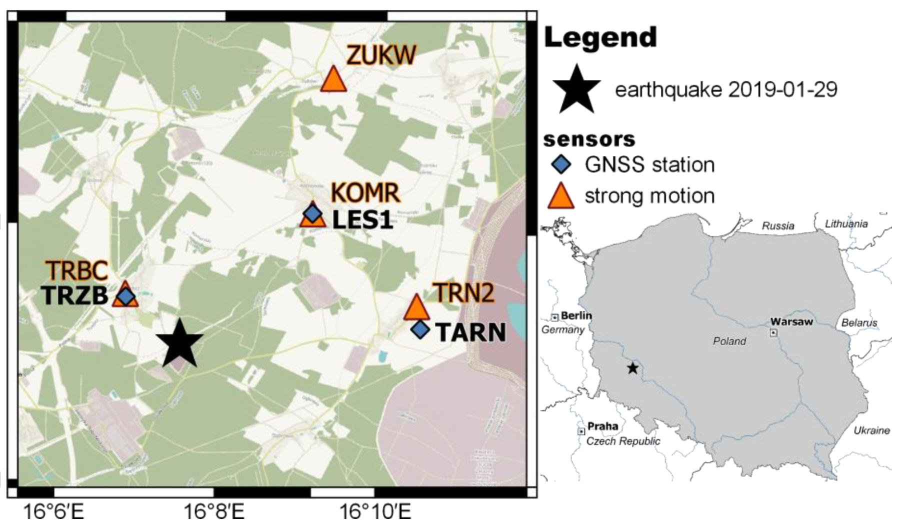

Figure 1: Distribution of the high-rate GNSS stations and the seismic stations in the proximity of the 2019 mining tremor.

Data processing scenario

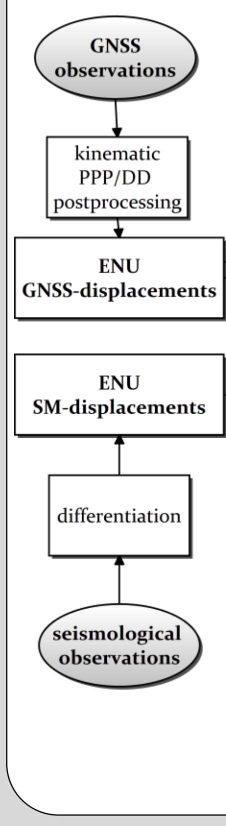

Processing with Precise Point Positioning (PPP) and Double Differencing (DD) approaches was prepared with final CODE orbit and clock products with RTKlib v2.4.3 and GAMIT software, respectively.

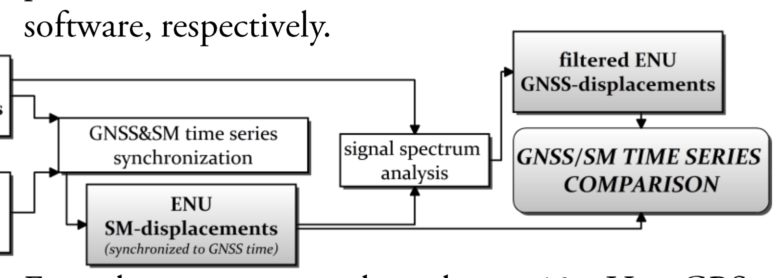

For this event two-hour-long 10 Hz GPS observations were processed. The sampling frequency of the TRZB and TARN stations was attenuated to 10 Hz. The original 50-Hz observations resulted in higher noise values, and for this event, such a high sampling frequency is irrelevant, as the spectral window of vibrations does not exceed 2.5 Hz.

Spectral window selection

The time series were reduced to one spectral window with 2nd-order Butterworth band-pass filter. We tested different frequency ranges to compromise the noise limitation and not losing the geophysical part of the signal.

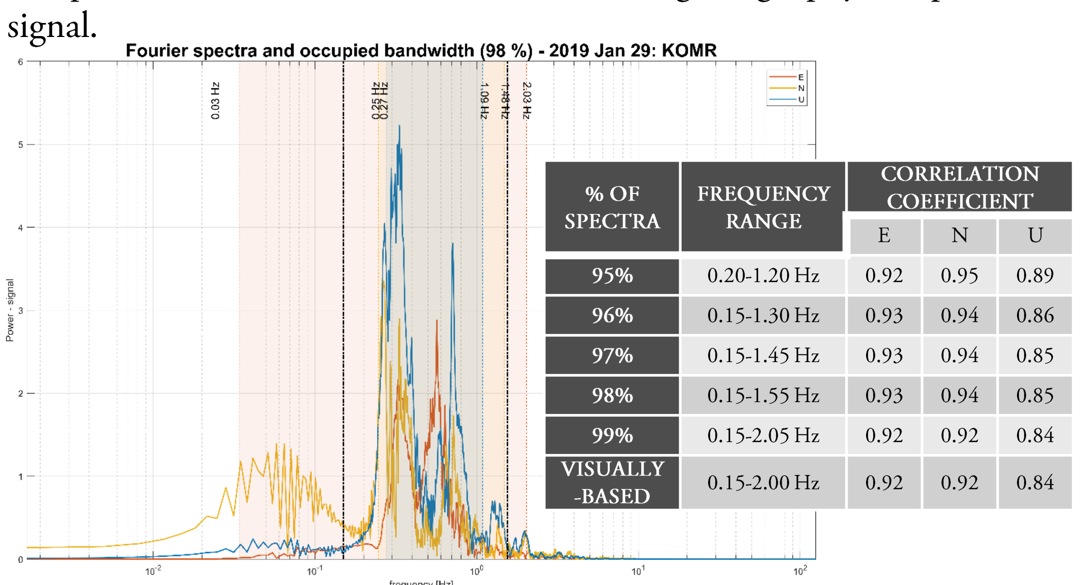

% OF SPECTRA	FREQUENCY RANGE	CORRELATION COEFFICIENT		
		E	N	U
95%	0.20-1.20 Hz	0.92	0.95	0.89
96%	0.15-1.30 Hz	0.93	0.94	0.86
97%	0.15-1.45 Hz	0.93	0.94	0.85
98%	0.15-1.55 Hz	0.93	0.94	0.85
99%	0.15-2.05 Hz	0.92	0.92	0.84
VISUALLY-BASED	0.15-2.00 Hz	0.92	0.92	0.84

Figure 2: Fourier spectra for displacement time series of seismic station KOMR with marked occupied bandwidth on 98% of spectra.

Table 2: List of correlation coefficients of PPP/SM displacement time series of KOMR /LES1 pair of sensors for different spectral windows.

The dominant frequencies of the DD and PPP approaches are consistent. For stations LES1 and TRZB, the spectral window was set to 0.15–2.00 Hz. Due to the different ground characteristics of the TARN station, for this station, the spectral window was limited to 0.15–1.20 Hz.

Agreement of high-rate GPS and seismological data

The time variability of Pearson's correlation coefficients of the GPS- and SM-displacement time series was examined with a 10-second moving window. In stable conditions, when no earthquake occurs, it is assumed that GPS- and SM-displacement time series should not be correlated and any increase in the correlation coefficient is random. However, during an event, the correlation should significantly increase.

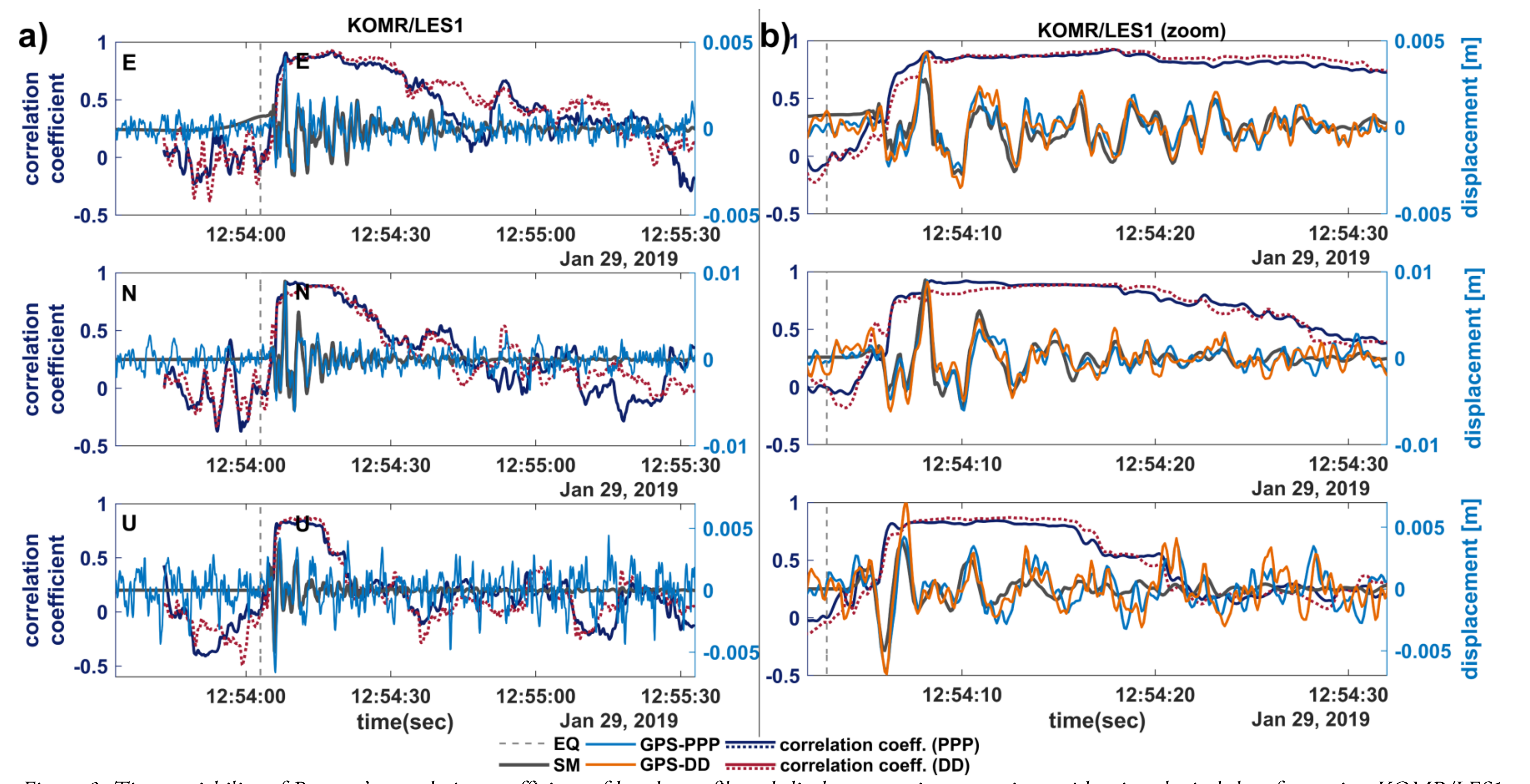

Figure 3: Time variability of Pearson's correlation coefficient of band-pass filtered displacements in comparison with seismological data for station KOMR/LES1. Left panel "a" presents 2-minute time series of SM and PPP-displacements. Right panel "b" presents 30-second time series of SM, PPP and DD-displacements. On both panels, the correlation coefficient variability for both solutions is presented.

The accuracy of GPS-derived displacements was verified with reference to seismological data. The similar values of PGD and amplitudes confirm the agreement presented with Pearson's correlation coefficient.

The consistency of the GPS- and SM-displacement time series in the frequency domain was assessed using coherence analysis in the common frequency range of 0–5 Hz. For all three sets of stations, for the less noiser horizontal components, there were two significant peaks of coherence values greater than 0.6 at frequencies 0.31–0.39 and 0.66–0.74 Hz.

APPROACH	GPS/SM STATION	PGD		AMPLITUDE (GPS)			AMPLITUDE (SM)			RMSE		
		GPS	SM	E	N	U	E	N	U	E	N	U
PPP	LES1/KOMR	9.0	9.0	6.6	15.0	11.1	5.5	14.8	8.8	0.5	1.0	1.3
PPP	TRZB/TRBC2	14.9	14.5	18.5	31.3	22.7	14.3	23.7	11.5	2.1	4.2	4.6
PPP	TARN/TRN2	8.5	2.2	11.7	11.0	16.6	4.1	2.8	2.8	1.3	1.7	2.3
DD	LES1/KOMR	8.8	9.0	7.8	15.0	14.1	5.5	14.8	8.8	0.6	1.2	1.4
DD	TRZB/TRBC2	8.1	14.5	12.8	15.9	10.8	14.3	23.7	11.5	0.8	1.8	1.8
DD	TARN/TRN2	8.5	2.2	12.6	11.4	16.6	4.1	2.8	2.8	1.3	1.8	2.4

Table 3: Peak ground displacements (PGD), peak-to-peak amplitudes (amplitude) and root mean square error (RMSE) of filtered PPP and DD displacements (mm).

GPS/SM STATION	SEPARATION [km]	DD/SM			PPP/SM		
		E	N	U	E	N	U
LES1/KOMR	0.002	0.93	0.89	0.87	0.92	0.92	0.84
TRZB/TRBC2	0.045	0.94	0.89	0.52	0.90	0.82	0.58
TARN/TRN2	0.316	0.66	0.55	0.70	0.70	0.61	0.62

Table 4: List of maximum correlation coefficients for PPP/SM and DD/SM band-pass filtered displacement time series.

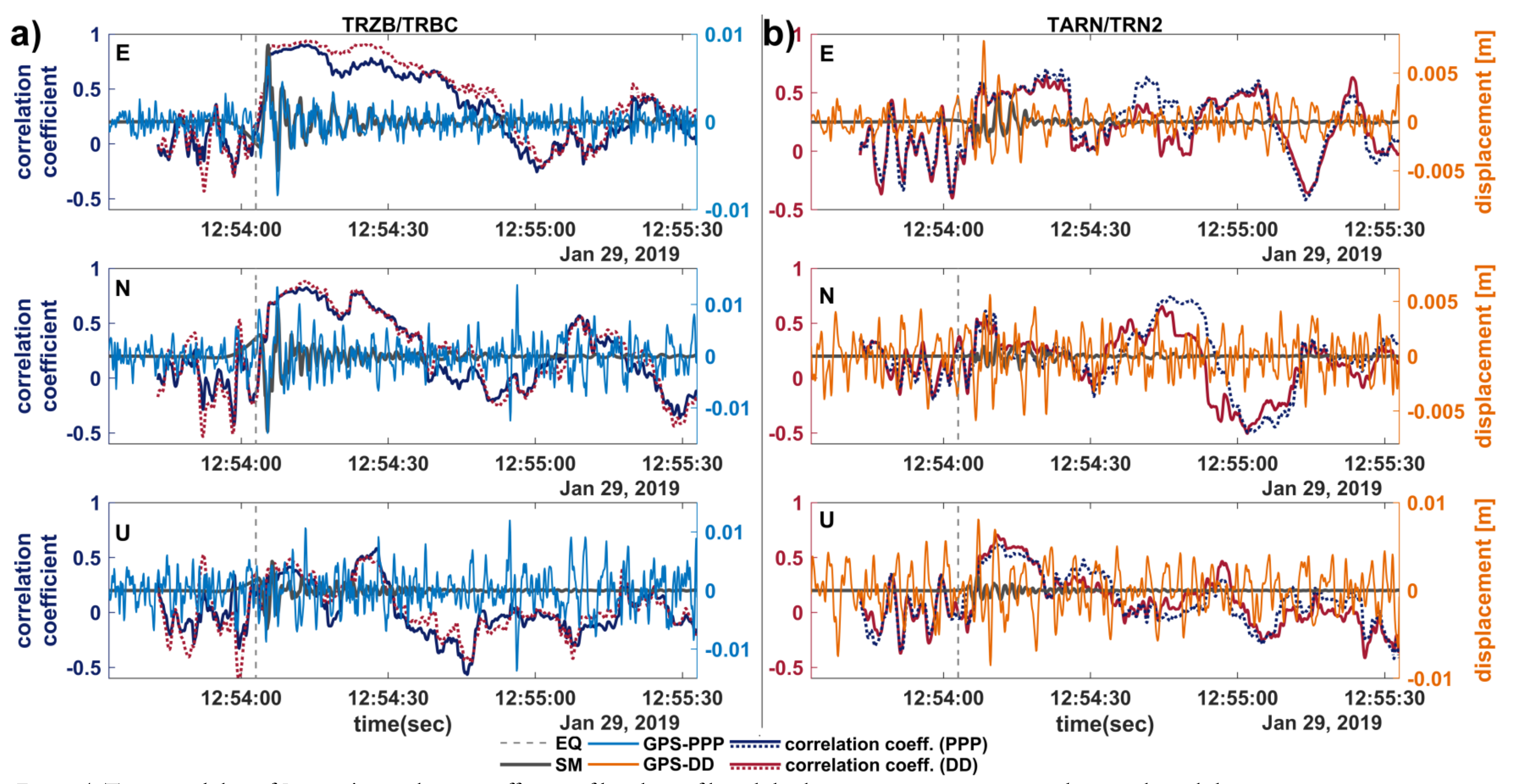

Figure 4: Time variability of Pearson's correlation coefficient of band-pass filtered displacements in comparison with seismological data on 2-minute time series. Left panel "a" presents PPP-displacements for station TRZB/TRBC and right panel "b" presents DD-displacements for station TARN/TRN2. On both panels, the correlation coefficient variability for both solutions is presented.

Detection of mining tremor in GPS displacement time series

We tested the time variability of mean, median, standard deviation (STD) and median absolute deviation (MAD) in a 10-second moving window, shifting every epoch, to investigate the mining tremor detection performance of GPS-displacement.

- The low frequencies are eliminated by filtering the median and mean coincide and oscillate around zero.
- STD and MAD coefficients rapidly increase, once the tremor occurs.
- The clarity of the increases in MAD and STD strongly depends on the noise level of the time series.
- For all three stations, the change in STD and MAD was the clearest in the East displacement time series.
- For the LES1 station even over a one-hour the increases in STD and MAD for the horizontal component are essential and make it possible to identify this event.

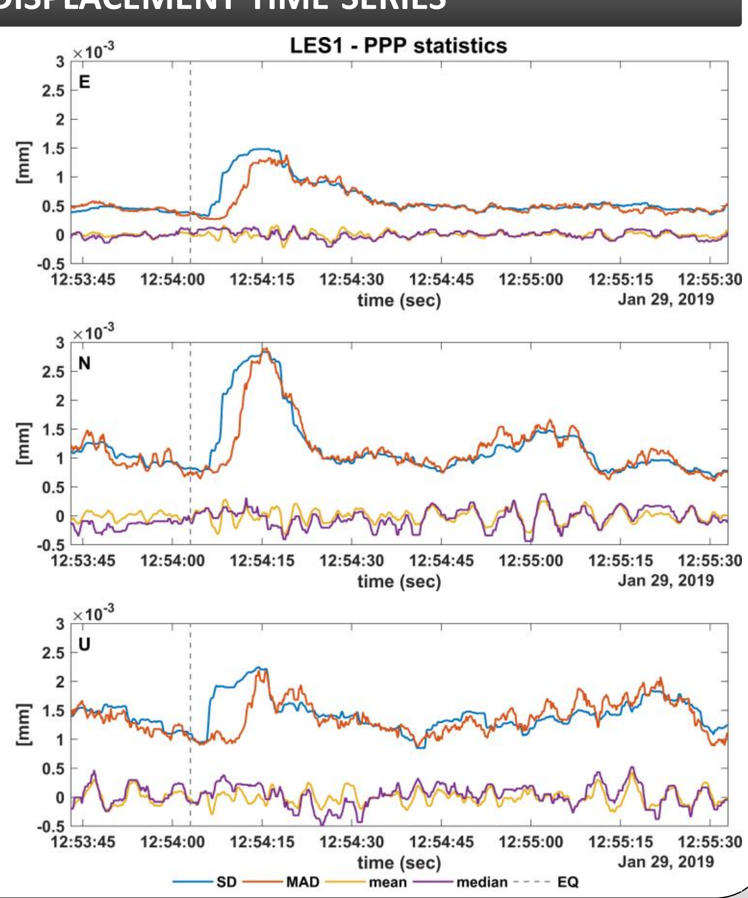

Figure 5: Statistics for the station LES1 2-minute band-pass filtered displacement time series calculated with the PPP approach.

Conclusion and perspectives

- ✓ To the best of our knowledge, this is the first study to analyse mining tremor using the high-rate GNSS technique, here limited to GPS data.
- ✓ In this mining tremor, the peak ground displacements reached 2-15 mm and show Pearson's correlation value in a range of 0.61 to 0.94 for band-pass filtered horizontal displacements.
- ✓ For the DD results, high-pass filtering is sufficient to obtain good agreement with seismological displacements, whereas, for the PPP results, reduction of high-frequency noise is also important.
- ✓ These results indicate that not only natural earthquakes of magnitudes over 5 can be analysed with GNSS technique, but smaller events might also be recorded with GPS receivers when the epicentral distance is shorter, benefiting of its high resistance to saturation.
- ✓ In mining areas, a dense network of low-cost GNSS receivers recording with a minimum frequency of 5 Hz would allow for more extensive analysis of post-mining ground deformations and could contribute to more accurate determination of event parameters.

Main references
- I. Kudlacik, J. Kapłon, J. Bosy, G. Lizurek, Seismic phenomena in the light high-rate GPS precise point positioning results, Acta Geodyn. Geomater. 193 (2019) 99–112. https://doi.org/10.13168/AGG.2019.0008.
- I. Kudlacik, J. Kapłon, G. Lizurek, M. Crespi, G. Kurpiński, High-rate GPS positioning for tracing anthropogenic seismic activity: the 29 January 2019 mining tremor in Legnica- Głogów Copper District, Poland; (2020) in review

Acknowledgements This work was carried out within EPOS – the European Plate Observing System, co-financed by the European Union from the funds of the European Regional Development Fund, POIR.04.02.00-14-A0003/16. Seismological data for this study was provided by the Institute of Geophysics, Polish Academy of Sciences. The GNSS data from the TRZB and TARN stations was provided courtesy of KGHM Cuprum Sp. z. o. o. and the University of Warmia and Mazury, co-financed by the National Centre for Research and Development, POIR.04.01.04-00-0056/17.